JOURNAL OF APPLIED ELECTROCHEMISTRY 23 (1993) 1056–1062

Kinetic model of anodic oxidation of titanium in sulphuric acid

B. J. HWANG*, J. R. HWANG

Department of Chemical Engineering, National Taiwan Institute of Technology, Taipei, Taiwan, 106 People's Republic of China

Received 13 October 1992; revised 20 January 1993

A kinetic model for the galvanostatic oxidation of titanium is proposed and compared with experimental results. The kinetic model takes account of the oxidation of titanium, the incorporation process, the evolution of oxygen, the avalanche process, the dissolution of titanium oxide and the capacitance effect of the double layer. The results indicate that the dissolution rate of titanium oxide is negligible and that the rate of oxygen evolution plays an important role in the anodic oxidation. The kinetic model is developed further for the following three special cases:

Case 1: when the anodization time approaches zero

$$dV/dt = K(I_t - I_0 - I_d)$$

Case 2: when the anodization time is larger than the transition time (τ)

$$dV/dt = K(I_t - I_e - I^*_{O_2} - I_d)$$

Case 3: when the anodization time is smaller than the transition time (τ)

$$dV/dt = K\left(I_t - I_e - \left(\frac{\xi t}{1+\xi t}\right)I^*_{O_2} - I_d\right)$$

where K and ξ are constants and $I_t, I_0, I_e, I^*_{O_2}$ and I_d are the applied current density, primary electron current density, rate of avalanche process, rate of oxygen evolution and dissolution rate of titanium oxide, respectively. The predictions of the proposed kinetic model correlate well with the experimental results.

Nomenclature

A_{Ti}	surface area of titanium (cm^2)
A_{TiO_2}	surface area of titanium oxide (cm^2)
A_0	initial area of titanium (cm^2)
C	capacitance of double layer ($mF\,cm^{-2}$)
E	anodization field ($V\,cm^{-1}$)
F	Faraday constant
I_0	primary electron current density ($mA\,cm^{-2}$)
I_1	partial current density due to the oxygen ions reacting with Ti or TiO ($mA\,cm^{-2}$)
I_2	partial current density due to the incorporation process ($mA\,cm^{-2}$)
I_C	partial current density due to the capacitance effect of the double layer ($mA\,cm^{-2}$)
I_d	the partial current density due to the film dissolution ($mA\,cm^{-2}$)
I_e	partial current density due to the avalanche process ($mA\,cm^{-2}$)
I_i	ionic or oxygen ion current density, $I_{O^{2-}}$ ($mA\,cm^{-2}$)
$I_{O^{2-}}$	partial current density due to the insertion of oxygen ions ($mA\,cm^{-2}$)
I_{O_2}	partial current density due to the evolution of oxygen ($mA\,cm^{-2}$)
$I^*_{O_2}$	partial current density due to the evolution of oxygen after the transition time ($mA\,cm^{-2}$)
I_t	applied current density ($mA\,cm^{-2}$)
I_{Ti}	current density through Ti surface ($mA\,cm^{-2}$)
I_{TiO_2}	current density through TiO_2 ($mA\,cm^{-2}$)
k	rate constant in Equation 5
K	a constant defined by $EM/(n\rho F + EMC)$
M	average molecular weight of the oxide species ($g\,mol^{-1}$)
n	equivalent charge transfer number
t	anodization time (min)
V	applied voltage (V)
x	film thickness (cm)

Greek symbols

α	impact ionization coefficient (cm^{-1})
β	ratio of the oxide thickness to the anodization voltage ($cm\,V^{-1}$)
ξ	a constant (min^{-1})
ρ	density of the oxide layer ($g\,cm^{-3}$)
τ	transition time (min)
γ_{Ti}	ratio of thickness and conductivity of titanium
γ_{TiO_2}	ratio of thickness and conductivity of titanium oxide
η	columbic efficiency for the oxygen evolution

* Corresponding author.

0021-891X

1. Introduction

Recently titanium oxides have generated considerable interest in the field of photo-electrode materials [1–3]. Passive titanium is very protective and resistant to corrosion in most aqueous solutions, particularly in chloride solutions. As a result, titanium and its alloys are used extensively in marine environments and the chemical industry. Since it is very important in applications, most of the recent studies [4–6] on titanium have been focused on the kinetics of anodic formation of titanium oxide. Sibert [7] has studied the current density–voltage characteristics during galvanostatic oxidation of titanium. Dyer and Leach [8] have employed an ellipsometric method to study the film growth on titanium during galvanostatic oxidation. Ohtsuka *et al.* [9] have also studied the film growth of anodic oxide by the ellipsometric technique. Albella *et al.* [10] have studied the kinetic model of the anodic oxidation of titanium; however, the evolution of oxygen is not considered in their model. Heakal *et al.* [11] have investigated the anodic dissolution of titanium oxide film in phosphoric acid solutions. They have concluded that the rate of change in film thickness is determined by the difference in the rate of film growth and film dissolution. Albella *et al.* [12, 13] have analysed the anodization curves for tantalum based on a model of anodization which explicitly takes account of the electrolyte incorporation and the avalanche process. Laitinen and Pohl [14] have studied the kinetics of oxide growth, considering the evolution of oxygen during potentiostatic polarization of lead in sulphuric acid solution. The proposed model for the gavanostatic oxidation of metals in the literature are summarized in Table 1. Although numerous kinetic models for the anodic oxidation of metals have been proposed, one or more important processes have been excluded in these models, as shown in Table 1.

Table 1. The proposed model of the anodic oxidation of metals in the literature

Metal	*Model*	*Without considering*	*Literature*
Ti	$I_t = I_i$	I_e, I_{O_2}, I_C	[7]
Ti	$I_t = I_i$	I_e, I_{O_2}, I_C	[11]
Ta	$I_t = I_i + I_e$	I_{O_2}, I_C	[12, 13]
Ta	$I_t = I_i$	I_e, I_{O_2}, I_C	[10]
Pb	$I_t = I_i + I_{O_2}$	I_e, I_C	[14]
Ti	$I_t = I_i + I_e + I_{O_2} + I_C$		this work

The results from our preliminary studies imply that the coulombic efficiency for oxygen evolution in the anodic oxidation of titanium is very high. However, none of the published models have taken this into account. The purpose of this work is therefore to develop a general model and compare it with experimental results for the anodic oxidation of titanium in sulphuric acid.

2. Theory

During galvanostatic polarization of titanium in sulfuric acid, the applied current density is I_t. As shown in Fig. 1, the following processes take place at the phase boundaries or inside the oxide layer.

(i) Insertion of oxygen into the TiO_2 surface: Because electrons are inserted parallel to the insertion of oxygen, the insertion and transport of oxygen ions [14] can be expressed as:

$$H_2O = O^{2-}(TiO_2, s) + 2H^+ \qquad (1)$$

where $O^{2-}(TiO_2, s)$ represents an oxygen ion on the

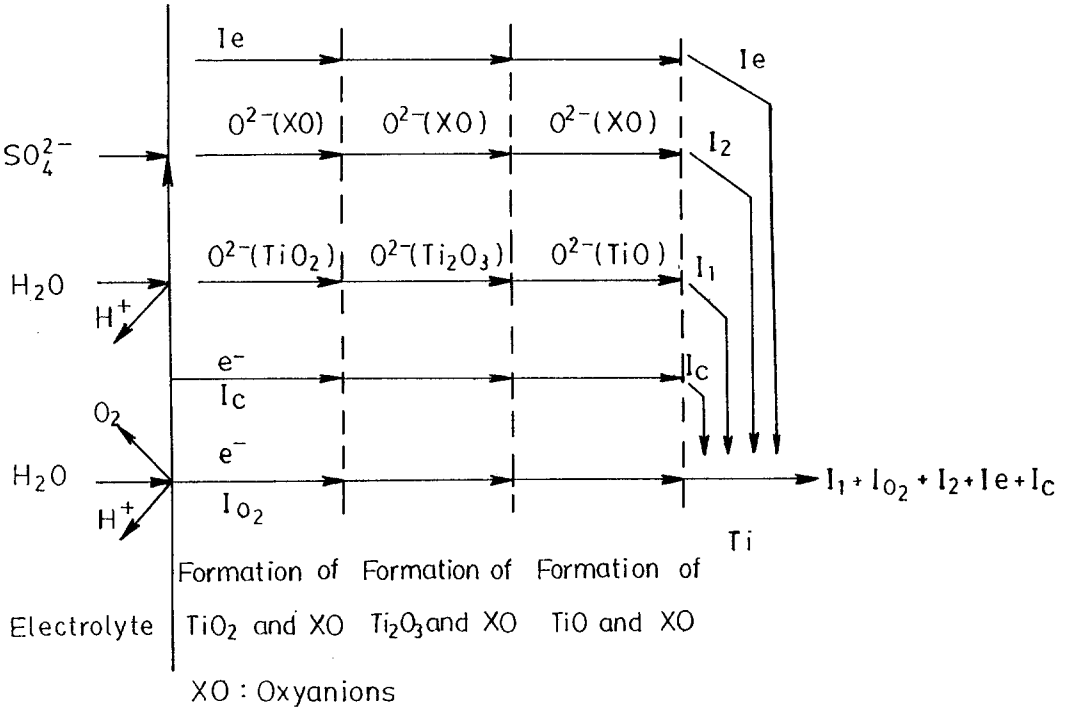

Fig. 1. Partial current density and reactions at the boundary or inside layer.

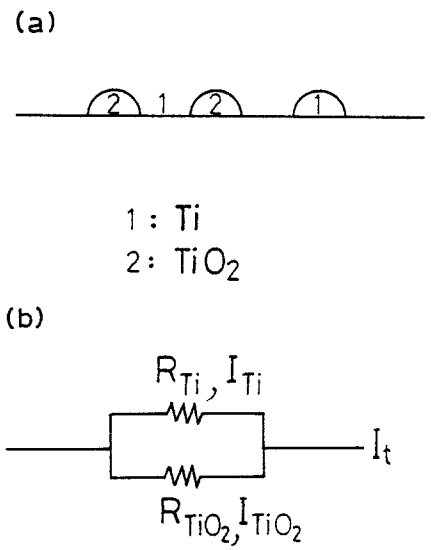

Fig. 2. (a) Surface condition during the initial stage of anodic oxidation. (b) Equivalent electric circuit.

TiO_2 surface. The partial current density due to this process is $I_{O^{2-}}$. Some of the oxygen ions generated within the oxide layer will react with TiO or Ti and the rest of the oxygen ions generated will be consumed in the incorporation process. The partial current densities are denoted as I_1 and I_2, respectively. The partial current density of the oxygen ion $I_{O^{2-}}$ can be expressed as

$$I_{O^{2-}} = I_1 + I_2 \tag{2}$$

(ii) Anodic evolution of gaseous oxygen at the TiO_2 surface:

$$2H_2O = O_2(g) + 4H^+ + 4e^-(TiO_2) \tag{3}$$

Before the anodization, the substrate surface is uniform and has no island of TiO_2. During the initial period of anodization, the surface becomes non-uniform, as shown in Fig. 2(a). We assume that gaseous oxygen is not generated and only oxygen ions are produced by Reaction 1 on the titanium surface. Both oxygen ions and gaseous oxygen are generated by Reactions 1 and 3 on the titanium oxide surface. Figure 2(b) represents the equivalent electric circuit of Fig. 2(a). The current through the titanium oxide (I_{TiO_2}) can be written as

$$I_{TiO_2}/I_t = \left(\frac{\gamma_{Ti}A_{TiO_2}}{\gamma_{TiO_2}A_{Ti}}\right) \Big/ \left(1 + \frac{\gamma_{Ti}A_{TiO_2}}{\gamma_{TiO_2}A_{Ti}}\right) \tag{4}$$

where γ_{Ti} and γ_{TiO_2} are the ratio of the thickness and the conductivity of titanium and titanium oxide, respectively. A_{Ti} and A_{TiO_2} are the surface area of the titanium and titanium oxide, respectively.

If the formation rate of titanium oxide surface is second order with respect to the titanium surface

$$dA_{TiO_2}/dt = kA_{Ti}^2 \tag{5}$$

where k is the reaction rate constant. Since

$$A_0 = A_{Ti} + A_{TiO_2} \tag{6}$$

where A_0 is the initial surface area of titanium.

Integrating Equation 5 yields

$$A_{TiO_2}/A_{Ti} = kA_0t \tag{7}$$

Substituting Equation 7 into Equation 4 gives

$$I_{TiO_2} = \frac{\xi t}{1+\xi t} I_t \tag{8}$$

where

$$\xi = (\gamma_{Ti}/\gamma_{TiO_2})kA_0 \tag{9}$$

If the coulombic efficiency for oxygen evolution is zero on the titanium surface and is constant on the titanium oxide surface, the partial current density for forming of gaseous oxygen is

$$I_{O_2} = \eta I_{TiO_2} \tag{10}$$

where η is the coulombic efficiency for oxygen evolution. After the transition time τ, the titanium surface is completely covered by the formation of titanium oxide. The current density through the TiO_2 surface, I_{TiO_2}, is I_t. The partial current for density gaseous oxygen formation, I_{O_2}, is independent of time and can be expressed as

$$I_{O_2} = I^*_{O_2} = \eta I_t \tag{11}$$

where $I^*_{O_2}$ is the partial current density of gaseous oxygen formation after the transition time.

Before the transition time τ, the coverage of TiO_2 is incomplete on the Ti surface. According to Equations 8, 10 and 11, the anodic evolution of gaseous oxygen can be expressed as

$$I_{O_2} = \frac{\xi t}{1+\xi t} I^*_{O_2} \tag{12}$$

where ξ is a constant at fixed applied current density and t is the anodization time. The partial current density of gaseous oxygen I_{O_2} depends on the coverage of titanium oxide on the titanium. The anodic evolution of gaseous oxygen increases with increasing TiO_2 coverage on the surface.

(iii) Avalanche process. The electronic current density grows exponentially with oxide thickness x and can be expressed as [15]

$$I_e = I_0 \exp(\alpha x) = I_0 \exp(\alpha\beta V) \tag{13}$$

where I_0 is the primary electron current density, α is the impact ionization coefficient and β is the ratio of the oxide thickness to the anodization voltage at a constant current density and is given by the inverse of the anodization field E, i.e. $\beta = 1/E$.

(iv) Dissolution of titanium oxide. The partial current density of dissolution is I_d.

(v) Capacitance effect of the double layer. This will consume part of the current density and can be expressed as

$$I_C = C\frac{dV}{dt} \tag{14}$$

where C is the average of double layer capacitance during the anodization process.

As a consequence, the continuity equation of current

density before the transition time is

$$I_t = I_{O^{2-}} + \frac{\xi t}{1+\xi t} I^*_{O_2} + I_e + I_C \quad (15)$$

Similarly, the continuity equation of current density after the transition time can be expressed as

$$I_t = I_{O^{2-}} + I^*_{O_2} + I_e + I_C \quad (16)$$

From the above considerations, it is obvious that the current density of oxygen ion $I_{O^{2-}}$ should follow Faraday's law and give rise to the film growth. The rate of change in film thickness is determined by the difference in the rate of film growth and film dissolution [11]

$$\frac{dx}{dt} = \frac{M}{n\rho F}(I_{O_2} - I_d) \quad (17)$$

where M is the average molecular weight of the oxide species, n is the equivalent charge transfer numbers, and F is the Faraday constant.

The electronic field E within the oxide layer can be considered as a constant [10]. Therefore, we have

$$x = V/E \quad (18)$$

Substituting Equation 18 into Equation 17 yields

$$\frac{dV}{dt} = \frac{EM}{n\rho F}(I_{O^{2-}-I_d}) \quad (19)$$

Combining Equations 13–16 and 19 leads to the following two possibilities:

(a) When the anodization time is smaller than the transition time τ,

$$\frac{dV}{dt} = K\left(I_t - I_0 \exp(\alpha\beta V) - \frac{\xi t}{1+\xi t} I^*_{O_2} - I_d\right) \quad (20)$$

where K is equal to $EM/(n\rho F + EMC)$.

(b) When the anodization time is larger than the transition time τ,

$$\frac{dV}{dt} = K(I_t - I_0 \exp(\alpha\beta V) - I^*_{O_2} - I_d) \quad (21)$$

The overall anodization process can be developed further for three special cases as follows,

Case 1: When the anodization time approaches zero, the evolution of oxygen does not occur on the titanium surface. As a consequence, the partial current density of gaseous oxygen formation and voltage are both equal to zero.

Equation 20 can be simplified to

$$\left(\frac{dV}{dt}\right)_0 = KI_t - K(I_0 + I_d) \quad (22)$$

Case 2: When the anodization time is larger than the transition time, the partial current density of gaseous oxygen formation is not changed. Equation 21 can be rewritten as

$$\ln\left(I_t - I^*_{O_2} - \frac{1}{K}\frac{dV}{dt}\right) = \ln I_0 + \alpha\beta V \quad (23)$$

Case 3: When the anodization time is smaller than the transition time, Equation 20 can be rearranged as

$$\frac{I^*_{O_2}}{I_t - I_0 \exp(\alpha\beta V) - I_d - (dV/dt)/K} = 1 + \frac{1}{\xi t} \quad (24)$$

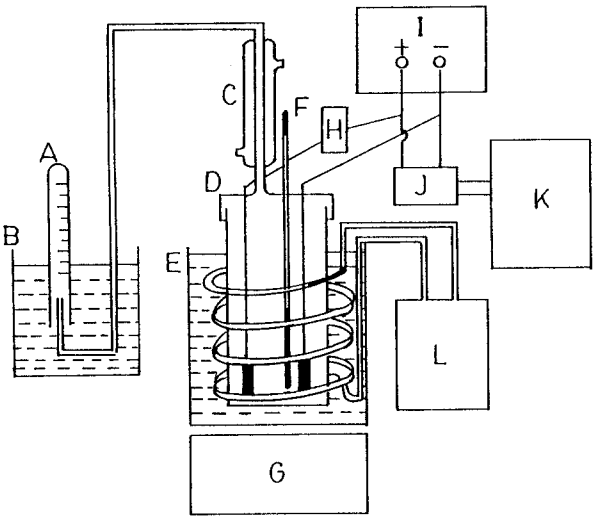

Fig. 3. Experimental apparatus for the anodic oxidation of titanium.

3. Experimental details

The titanium electrode was made from a commercially available titanium sheet of purity above 99.5%. The specimens were etched with a mixture of HF (48 wt %) and HNO_3 (70%) in the volume ratio 1 to 3 for 30 s at room temperature and then rinsed with distilled water. The anodic electrode surface was fixed with Epofix epoxy resin and Epofix hardener reagents in the volume ratio 15 to 2(Struers), leaving a desired surface area in contact with the electrolytes. Solution containing 0.5 M sulphuric acid were prepared from reagent grade chemicals and distilled water. The specimen was activated in the etching solution for 30 s.

The experimental setup is shown in Fig. 3. The closed electrolytic cell (C) was a 300 ml cylindrical glass vessel in a water bath (E) equipped with a heating coil. The thermostated water (L) was circulated through the coil to control the temperature of solution at 293 ± 0.5 K. A platinum foil of about 4 cm^2 area was used as the counter electrode for anodization. Anodic oxidation was carried out using a power supply (I). The voltage was recorded by a versatile computer recorder (K). The charge was measured with a coulometer (H) during the anodization. The gas evolved from the anode and cathode was collected through a gas collector (A). The amount of titanium ions dissolved into solution during the anodization was determined by atomic absorption spectroscopy.

4. Results and discussion

4.1. *Transient voltage*

The anodic oxidation of titanium was carried out at various current densities. Figure 4 shows the results of some typical runs. In the initial stage, the voltage increases sharply indicating rapid film growth. The rate of voltage change stays almost constant. Later, the rate of voltage change decreases with time. The rate of voltage change increases with increasing

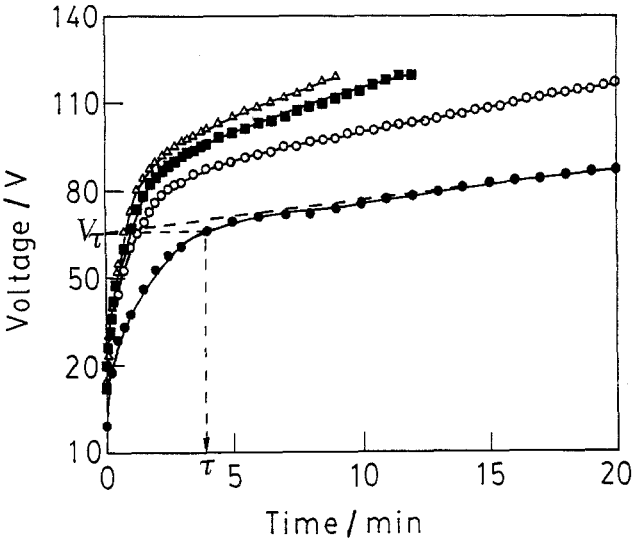

Fig. 4. Transient of voltage at different current densities. Operation conditions: 0.5 M H_2SO_4; $T = 20\,°C$. Current density: (●) 5.00, (○) 7.19, (■) 9.48, (△) 11.0 mA cm^{-2}.

current density during the initial stage, as shown in Fig. 4. The voltage (V_τ) at the transition time can be obtained by the intercept of the straight line. The transition time (τ) can be obtained from the transition voltage (V_τ), as shown in Fig. 4. The transition times determined at various current densities are shown in Table 2. The transition time decreases with increasing current density. This suggests that the titanium surface is completely covered more rapidly by titanium oxide as the current density increases. The plot of transition time against the inverse of current density is shown in Fig. 5. The results give a straight line and can be expressed as

$$\tau = 21.3/I_t \qquad (r^2 = 0.97) \qquad (25)$$

This implies that the titanium is completely covered by titanium oxide at constant charge passed.

4.2. *Dissolution rate of titanium oxide*

The dissolution rate of titanium oxide was obtained by analyzing the terminal concentration of titanium ions in solution using atomic absorption spectroscopy. The average partial current density of dissolution is about 2.08×10^{-3} mA cm^{-2}. The partial current density of film dissolution (I_d) can be neglected when compared with other terms in the current density continuity equation.

Table 2. The parameters of the proposed kinetic model at various current densities
Operation conditions: 0.5 M H_2SO_4; $T = 20\,°C$

I_t /mA cm^{-2}	I_0 /mA cm^{-2}	$\alpha\beta \times 10^{-4}$ /V^{-1}	ξ /min^{-1}	τ /min
11.62	1.06	31.9	9.8	1.2
11	0.97	37.7	11.23	1.7
9.48	0.93	21.6	9.20	2.0
7.19	1.14	6.57	6.4	2.8
5.88	0.83	5.73	6.45	3.8
5.00	0.82	5.65	7.57	3.9
2.91	1.14	4.39	6.21	7.8

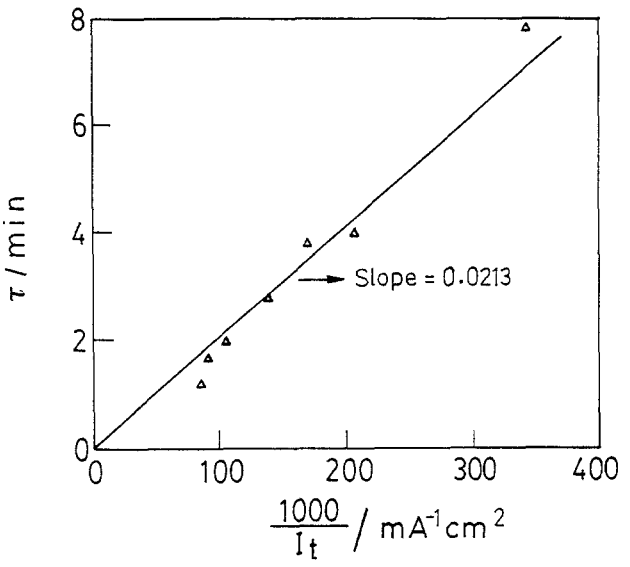

Fig. 5. Plot of transition time against $1/I_t$. Operation conditions: 0.5 M H_2SO_4; $T = 20\,°C$.

4.3. *Transient gas evolution*

The total gas evolution, including both hydrogen and oxygen, was collected by the gas collector during anodization. The evolution of hydrogen was calculated by measuring the charge passed during anodization. The evolution of oxygen was calculated as the difference between the total gas measured and the hydrogen. Typical results are shown in Fig. 6. When the anodization time is large, the amount of oxygen evolution increases linearly with the anodization time, as shown in Fig. 6. The oxygen partial current density $I^*_{O_2}$ was obtained from the rate of oxygen evolution. Figure 7 shows the relationship between current density and the oxygen partial current density $I^*_{O_2}$. The results indicate that $I^*_{O_2}$ increases with increasing applied current density and

$$I^*_{O_2} = 0.85\, I_t \qquad (r^2 = 0.99) \qquad (26)$$

The coulombic efficiency (η) for oxygen evolution was

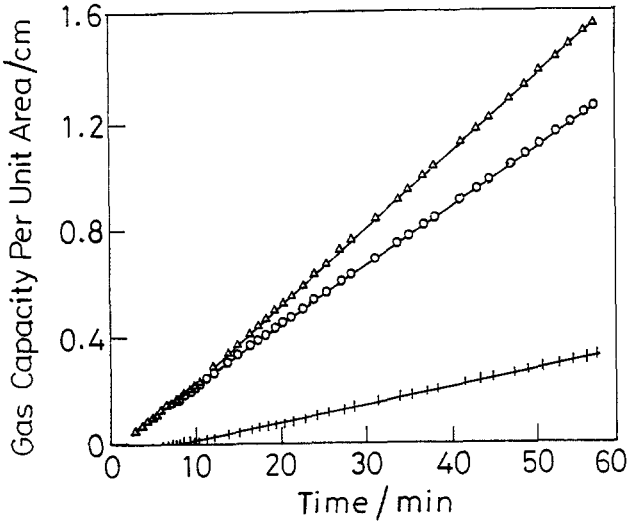

Fig. 6. Gas capacity against time during anodization. Operation conditions: 0.5 M H_2SO_4; $T = 20\,°C$; c.d. = 2.91 mA cm^{-2}. (△) Total gas; (○) H_2 and (+ + +) O_2.

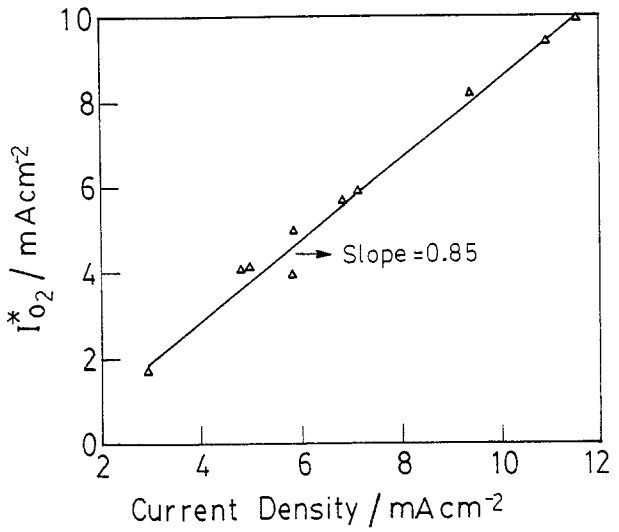

Fig. 7. Partial current density of gaseous oxygen against applied current density. Operation conditions: 0.5 M H_2SO_4; $T = 20\,°C$.

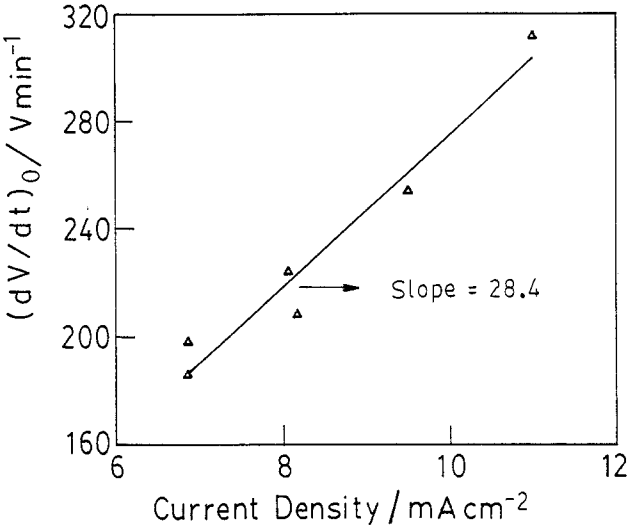

Fig. 8. Plot of $(dV/dt)_0$ against I_t. Operation conditions: 0.5 M H_2SO_4; $T = 20\,°C$.

0.85. This implies that 85% of applied current density is consumed by oxygen evolution after the transition time.

4.4. *Analysis of kinetic model*

Three cases may be considered:

(*Case 1*) When the anodization time approaches zero, the voltage approaches zero and evolution of gaseous oxygen does not occur on the titanium surface. The initial rate of voltage change $(dV/dt)_0$ at various current densities can be obtained from Fig. 4. The plot of $(dV/dt)_0$ against current density I_t is shown in Fig. 8. The results indicate that the initial rates of voltage change increase linearly with current density and the slope is 28.4. The results are consistent with Equation 22. Comparing the slope of the line in Fig. 8 and Equation 22, the constant K can be obtained as 2.87 V cm^2 mA^{-1} min^{-1}.

(*Case 2*) When the anodization time is larger than the transition time, the partial current density of gaseous oxygen formation is constant. The rate of voltage change (dV/dt) at different voltages can be obtained from Fig. 4. The plot of $\ln(I_t - I^*_{O_2} - I_d - dV/K dt)$ against voltage at 9.48 mA cm^{-2} is shown in Fig. 9. The results indicate that the term $\ln(I_t - I^*_{O_2} - I_d - dV/dt)$ is proportional to the voltage. This is consistent with Equation 23. Based on the slope and intercept of Fig. 9 and Equation 23, the parameters $\alpha\beta$ and I_0 are 2.165×10^{-3} V^{-1} and 0.927 mA cm^{-2}, respectively.

(*Case 3*) When the anodization time is smaller than the transition time, the rate of gaseous oxygen evolution increases with time. Similarly, the plot of $I^*_{O_2}/(I_t - I_0 \exp(\alpha\beta V) - I_d - dV/K dt)$ against $1/t$ at 9.48 mA cm^{-2} results in a straight line, as shown in Fig. 10. The results are consistent with Equation 24. Based on the slope of the straight line in Fig. 10 and Equation 24, the value of ξ is 9.20 min^{-1} at 9.48 mA cm^{-2}.

Similarly, the model parameters at various current densities can be obtained as shown in Table 2.

4.5. *Comparison between the experimental results and model calculation*

At 9.48 mA cm^{-2}, a typical result for voltage against

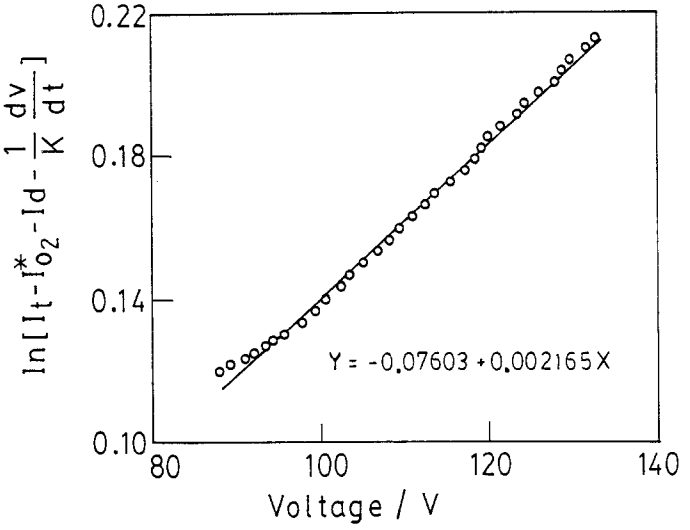

Fig. 9. Plot of $\ln(I_t - I^*_{O_2} - I_d - dV/K dt)$ against V. Operation conditions: 0.5 M H_2SO_4; $T = 20\,°C$; c.d. = 9.48 mA cm^{-2}.

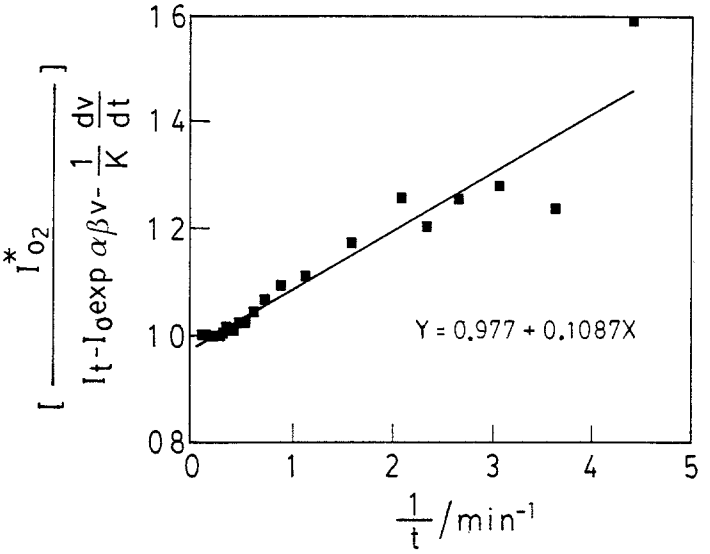

Fig. 10. Plot of $I^*_{O_2}/(I_t - I_0 \exp(\alpha\beta V) - dV/K dt)$ against $1/t$. Operation conditions: 0.5 M H_2SO_4; $T = 20\,°C$; c.d. = 9.48 mA cm^{-2}.

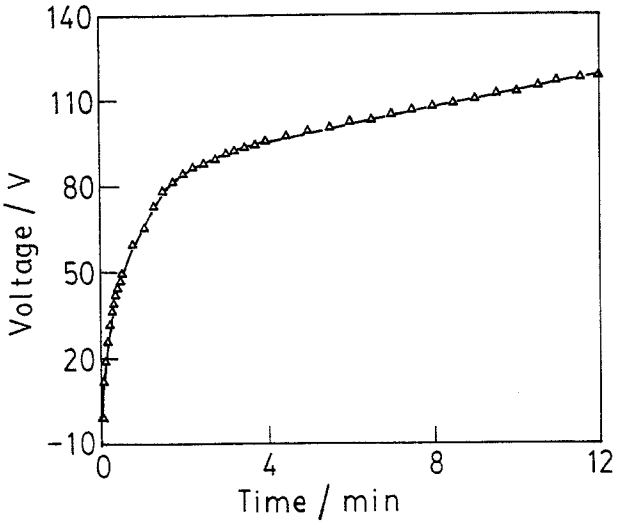

Fig. 11. Comparison between the experimental results (△) and calculation of the proposed kinetic model (– – –). Operation conditions: 0.5 M H_2SO_4; $T = 20\,°C$; c.d. = 9.48 mA cm^{-2}.

anodization time is shown in Fig. 11. The results of model calculation in Fig. 11 are obtained by substituting the parameters given in Table 2 into Equations 23 and 24. Based on the results of Fig. 11, the experimental results correlate very well with the calculations of the proposed kinetic model. Similarly, the results of model calculation also correlate well with the experimental results at other current densities.

Acknowledgement

The support of the National Science Council (NSC 79-0410-E011-02) and National Taiwan Institute of Technology of the Republic of China are acknowledged.

References

[1] M. R. Kozlowski, P. S. Tyler, W. H. Smyrl and R. T. Atanasoski, *J. Electrochem. Soc.* **136** (1989) 442.
[2] T. Yoko, A. Yuasa, K. Kamiya and S. Sakka, *ibid.* **138** (1991) 2279.
[3] R. W. Matthews, *J. Phys. Chem.* **91** (1987) 3328.
[4] W. Mizushima, *J. Electrochem. Soc.* **108** (1961) 825.
[5] R. S. Alwitt and K. Vijh, *ibid.* **116** (1969) 388.
[6] A. J. Aladjen, *Mater. Sci.* **8** (1973) 688.
[7] M.E. Sibert, *J. Electrochem. Soc.* **110** (1963) 65.
[8] C. K. Dyer and J. S. Leach, *ibid.* **125** (1978) 1032.
[9] T. Ohtsuka, M. Masuda and N. Sato, *ibid.* **132** (1985) 787.
[10] J. M. Albella, I. Montero, O. Sanchez and J. M. Martinez-Duart, *ibid.* **133** (1986) 876.
[11] F. E. Heakal, A. S. Mogoda, A. A. Mazhar and M. S. El-Basiouny, *Electrochim. Acta* **27** (1987) 453.
[12] J.M. Albella, I. Montero and J. M. Martinez-Duart, *J. Electrochem. Soc.* **131** (1984) 1101.
[13] J. M. Albella, I Montero and J. M. Martinez-Duart, *Thin Solid Films* **125** (1985) 57.
[14] T. Laitinen and J. P. Pohl, *Electrochim. Acta* **34** (1989) 377.
[15] S. Ikonopisov, *ibid.* **22** (1977) 1077.